

Annealing of Commercial Block Polypropylene.

I. Thermal and Physical Properties

JUN-ICHI ITO,* KATSUO MITANI, and YUKIO MIZUTANI

Fujisawa Laboratory, Tokuyama Soda Co., Ltd., 2051 Endo, Fujisawa City, Kanagawa 252, Japan

SYNOPSIS

Investigations were carried out regarding the effect of annealing of ethylene-propylene block copolymer (block PP) moldings on their tensile impact strength (TIS), brittle temperature (T_b), and other mechanical properties. Annealing near the melting point improves TIS and T_b as the result of recrystallization. With a system in which a minute amount of talc is added as a nucleating agent, the degree of improving TIS through annealing is considerably less than that with a nonnucleated system. The effect of annealing on the impact strength is due to changes of fine texture and morphology of crystallites and is explicable by recrystallization and polymer diffusion. © 1992 John Wiley & Sons, Inc.

INTRODUCTION

Polypropylene (PP) has various excellent properties as a general purpose resin, such as thermal resistance, rigidity, and chemical resistance. However, its greatest disadvantages are its low impact strength and high T_b temperature, which can be improved by copolymerization with another olefin (generally with ethylene) or blending with an elastomer, with inevitably decreasing the high rigidity characteristics of PP.

We have already proposed that annealing of PP blends after their molding is effective as a means of improving impact strength and T_b without sacrificing rigidity.^{1,2} There have also been reported some similar studies.^{3,4}

Commercial block polypropylenes have been produced through the first-stage polymerization to give a homo-PP or a random copolymer of propylene with a small amount of ethylene, followed by the second stage to effect copolymerization of propylene and ethylene. In some cases, a small amount of polyethylene (PE) has been produced in the second-stage polymerization. Accordingly, a block PP can be regarded as a highly complicated composite of polypropylene, poly(ethylene-co-propylene) (PEP), and polyethylene.⁵⁻⁷

In the present report, in the same way as with the study on PP blends, we studied the annealing effect on several commercial block PPs regarding mechanical properties and morphology.

EXPERIMENTAL

All polymers used were block PPs produced by Tokuyama Soda Co., among which block PP-A and PP-B were of commercial grade and PP-C was a special sample of high ethylene content prepared under similar condition. Table I shows compositions and properties of the polymers, of which characterizations were conducted in the same manner as in the previous report¹ in accordance with ASTM-D1822 and ASTM-D746. The values of TIS in Table I indicate the average of 10 measurements ($n = 10$). The standard deviations of TIS values were less than 10% of the average values. The values of T_b were determined by the statistical law with the data measured at least at five different temperatures. Other values in Table I were the average of the data measured with five test specimens. Measurement of isothermal crystallization velocity was made by a differential scanning calorimeter (Perkin-Elmer Co., Model DSC-1B), by first melting the sample in the DSC sample holder at 230°C for 10 min, cooling it to 120°C at a rate of 80°C/min, and then observing exothermal peaks. Observation of the fracture sur-

* To whom correspondence should be addressed.

Table I Mechanical Properties of Annealed Commercial Block PP

Sample	Annealing Condition	TIS (kg cm/cm ²)	Tb (°C)	YS (kg/cm ²)	TS (kg/cm ²)	$E \times 10^{-3}$ (kg/cm ²)	Elong. (%)	H_R	Crystallinity ^d (%)
Block PP-A ^a	Unannealed	70	-0.5	238	346	2.7	960	85	56.8
	Annealed (110°C, 3 h)	90	—	265	306	3.0	840	—	58.2
	Annealed (140°C, 3 h)	121	-9.0	265	310	3.2	820	88	59.7
Block PP-B ^b	Unannealed	66	-4.5	257	258	3.6	750	93	57.7
	Annealed (140°C, 3 h)	80	-9.5	241	224	4.6	270	95	65.3
Block PP-C ^c	Unannealed	95	-31.0	218	319	3.1	710	88	54.4
	Annealed (110°C, 3 h)	116	—	216	216	3.2	590	—	58.5
	Annealed (140°C, 3 h)	122	-33.0	218	220	3.3	320	89	61.6

^a Block PP-A: MFI = 6.0 g/10 min; ethylene content = 6.2 wt %; talc content = 0 wt %.

^b Block PP-B: MFI = 6.0 g/10 min; ethylene content = 6.2 wt %; talc content = 0.3 wt %.

^c Block PP-C: MFI = 5.7 g/10 min; ethylene content = 12.0 wt %; talc content = 0.35 wt %.

^d Measured by X-ray diffraction.

faces of the TIS test pieces was usually conducted immediately after property measurement by a scanning electron microscope (SEM). The *n*-heptane-extraction of the fracture surface of the TIS specimen was carried out with a Soxhlet extractor for 13 h under nitrogen.

RESULTS AND DISCUSSION

Effects of Annealing Temperature and Annealing Time

Table I summarizes the mechanical properties of the three types of block PPs. Based on these data, the effect of annealing on the mechanical properties of block PPs will be discussed regarding the effects of annealing temperature, talc addition, and ethylene content.

Figure 1 shows the annealing temperature and annealing time on TIS and crystallinity of block PP-A. The values of TIS and crystallinity are saturated in a few hours of annealing and increase at higher temperature.

The test pieces used in Table I and Figure 1 were prepared at different times of the year and the temperature of the cooling water for the compression-molding also varied. The values of TIS and crystal-

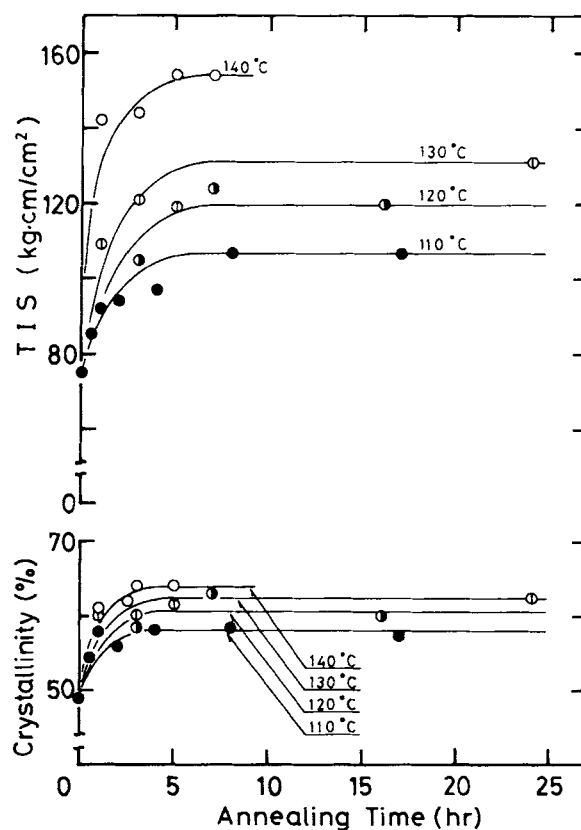


Figure 1 Dependence of TIS and crystallinity of block PP-A on the annealing temperature and time.

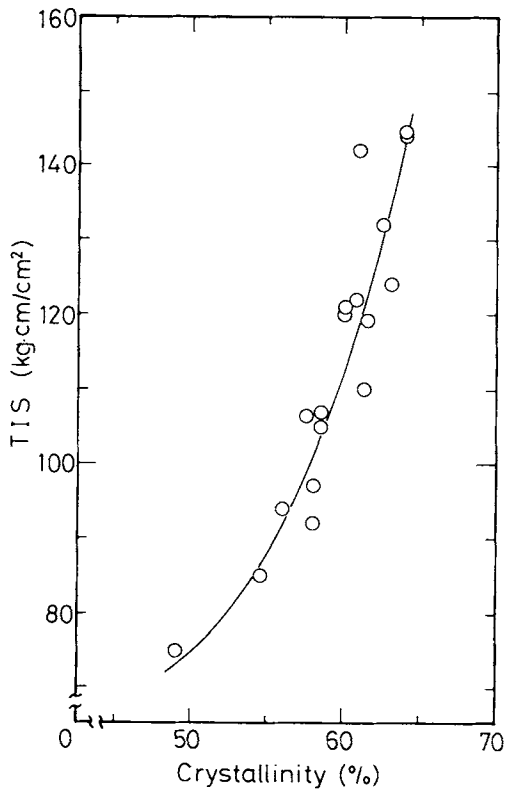


Figure 2 Relationship between TIS and crystallinity in block PP-A. (TIS vs. crystallinity were plotted with all data of Fig. 1.)

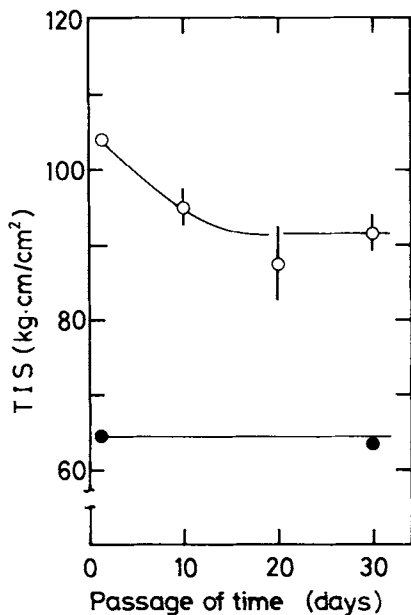


Figure 3 Change of TIS of block PP-A annealed at 140°C for 5 h with the passage of time. TIS test pieces were stored under 23°C and 50% RH: (●) unannealed; (○) annealed.

linity in Table I are, consequently, a little different from those in Figure 1.

With the block PP-A not containing talc, annealing effected increases in TIS (Fig. 1), T_b , yield strength (YS), elastic modulus (E), and Rockwell hardness (H_R) of the polymer with an increase in its crystallinity, in the same manner as with annealing of the PP/PEP blend. On the other hand, decreases in tensile strength (TS) and elongation (Elong.) are observed (see Table I).

Figure 2 indicates the relationship between TISs and crystallinities derived from the data in Figure 1 and suggests that the annealing effect of a block PP on its impact strength is closely related to the change in its crystal structure caused by annealing.

Figure 3 shows the time dependency of TIS when a block PP-A after annealing was allowed to stand at a room temperature. The TIS decreases by about

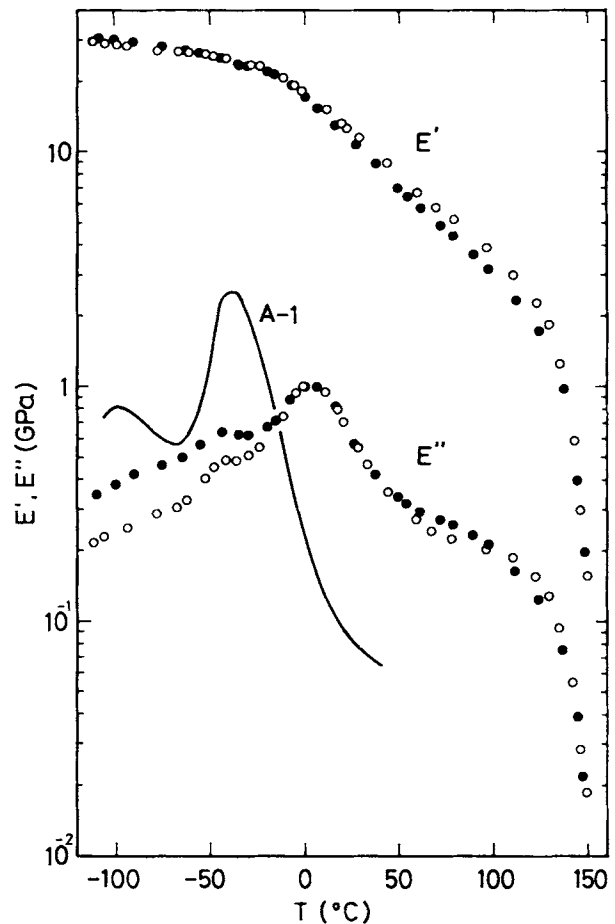


Figure 4 Dynamic viscoelastic properties of block PP-A: (●) unannealed; (○) annealed at 140°C for 3 h; a solid line shows E'' of the polymer (A-1) extracted with *n*-heptane from unannealed block PP-A.

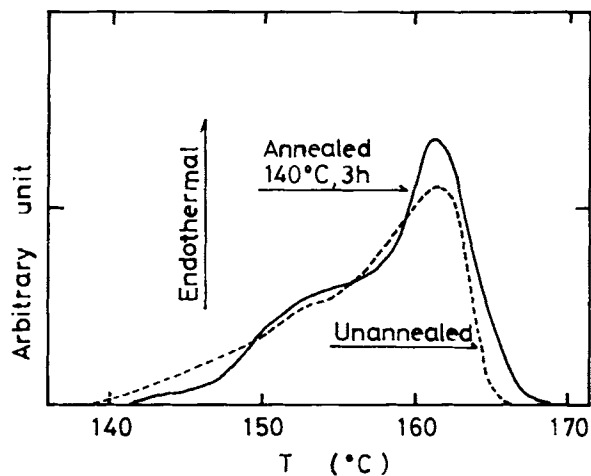


Figure 5 Normalized DSC curves of TIS test pieces of block PP-A (heating rate = 10°C/min): dashed line shows an unannealed sample (17.4 cal/g); solid line shows the sample annealed at 140°C for 3 h (19.6 cal/g).

10% in about 15 days, but is then stabilized, suggesting that the annealing effect is a partially irreversible phenomenon.

The above results are analogous to the annealing effects observed with the PP/PEP and PP/PE systems as reported in the preceding reports,^{1,2} suggesting the possibility of a similar discussion for the case of block PP.

Figure 4 shows the data of measurement of the dynamic viscoelastic property. Although an increase in the dynamic storage modulus E' is observed at above room temperature, no distinct change can be observed at the temperature for the peak dynamic loss modulus E'' . In other words, although an in-

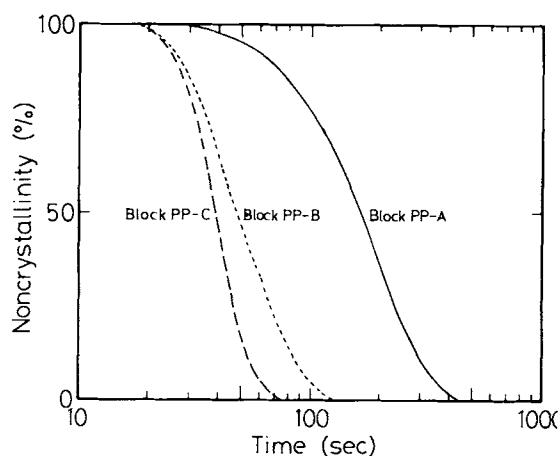


Figure 6 Crystallization velocity of each block PP at 120°C with DSC.

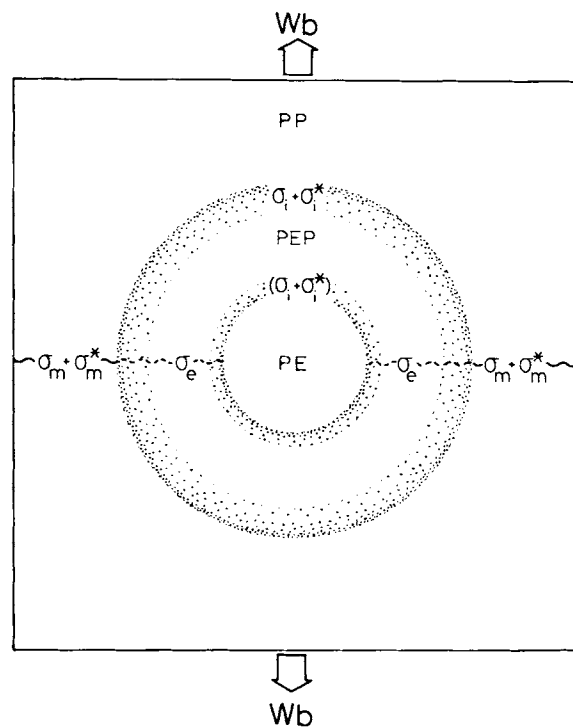


Figure 7 Fracture model for the annealing effect on TIS and T_b of block PP. The sizes of core and shell represent those of block PP-A. The dots at the PP/PEP and PEP/PE interfaces show the concentration of PEP crystal in the transitional layer formed by annealing.

crease in rigidity due to the progress of crystallization caused by annealing is observed in terms of viscoelasticity, the glass transition behaviors of PP

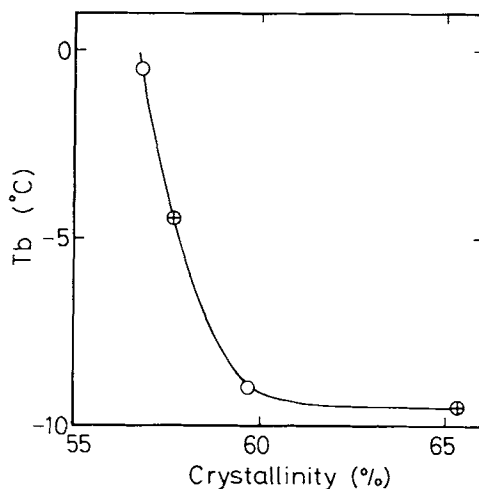


Figure 8 Relationship between T_b and crystallinity in block PP-A and -B: (○) block PP-A; (⊕) block PP-B. The data in Table I were plotted.

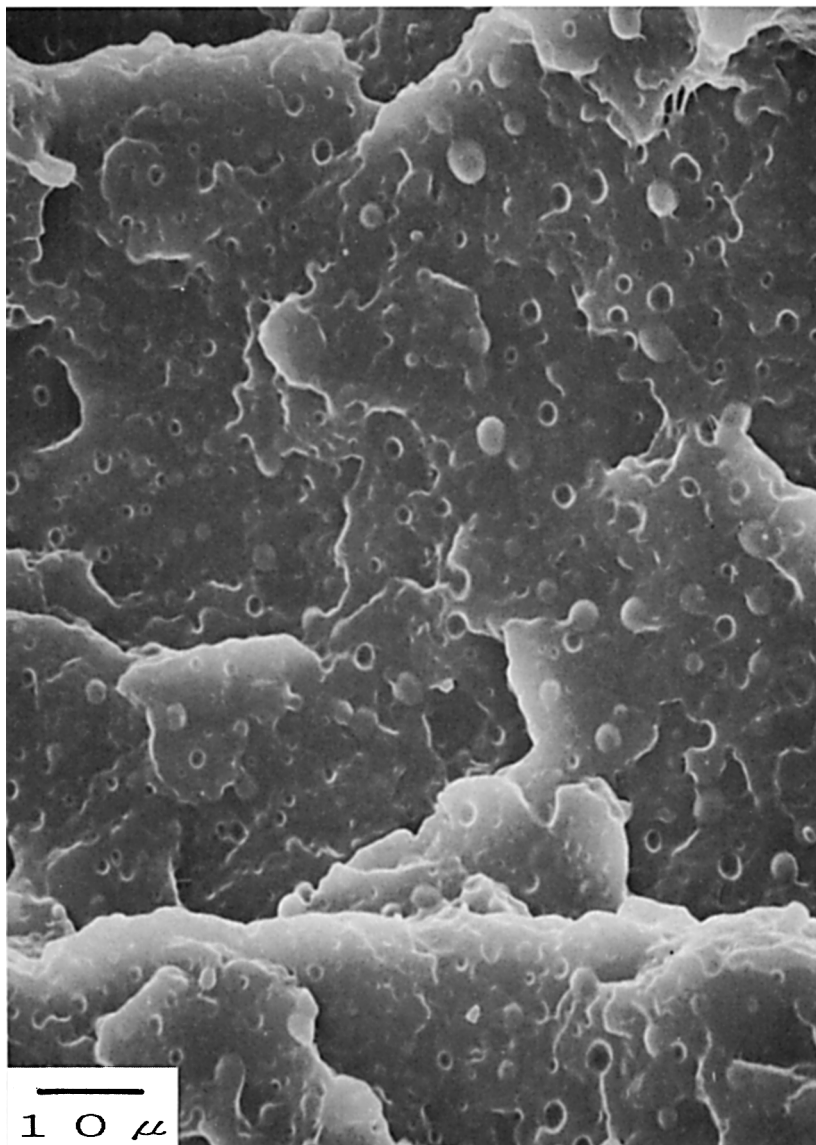


Figure 9 SEM of fracture surfaces of TIS test pieces for block PP-A: (a) unannealed; (b) annealed at 140°C for 3 h; (c) sample (a) extracted with *n*-heptane; (d) sample (b) extracted with *n*-heptane. The extraction was carried out in a Soxhlet extractor for 13 h under nitrogen.

or PEP could not be determined from the measurements in the present study.

Figure 5 illustrates the DSC curve for melting of a TIS test piece of the block PP-A. The enthalpies of fusion for the unannealed and annealed test pieces are 17.4 cal/g and 19.6 cal/g, respectively. It is found that annealing effected the shift of endothermal peaks toward higher temperature and the establishment of bimodality of the fusion profile, indicating the occurrence of the growth and thickening of lamella crystals of PP.

Annealing Effect for Talc-Added System

(a) Influence of Talc Addition

When a small amount of talc is added to PP, it functions as a nucleating agent to promote nucleation: producing a large number of nuclei, hence, micronizing the crystallites and increasing the crystallization velocity as a whole. The merits of the talc addition usually are as follows: improvement of clarity due to micronization of crystallites, shortening of the molding cycle, and improvements in

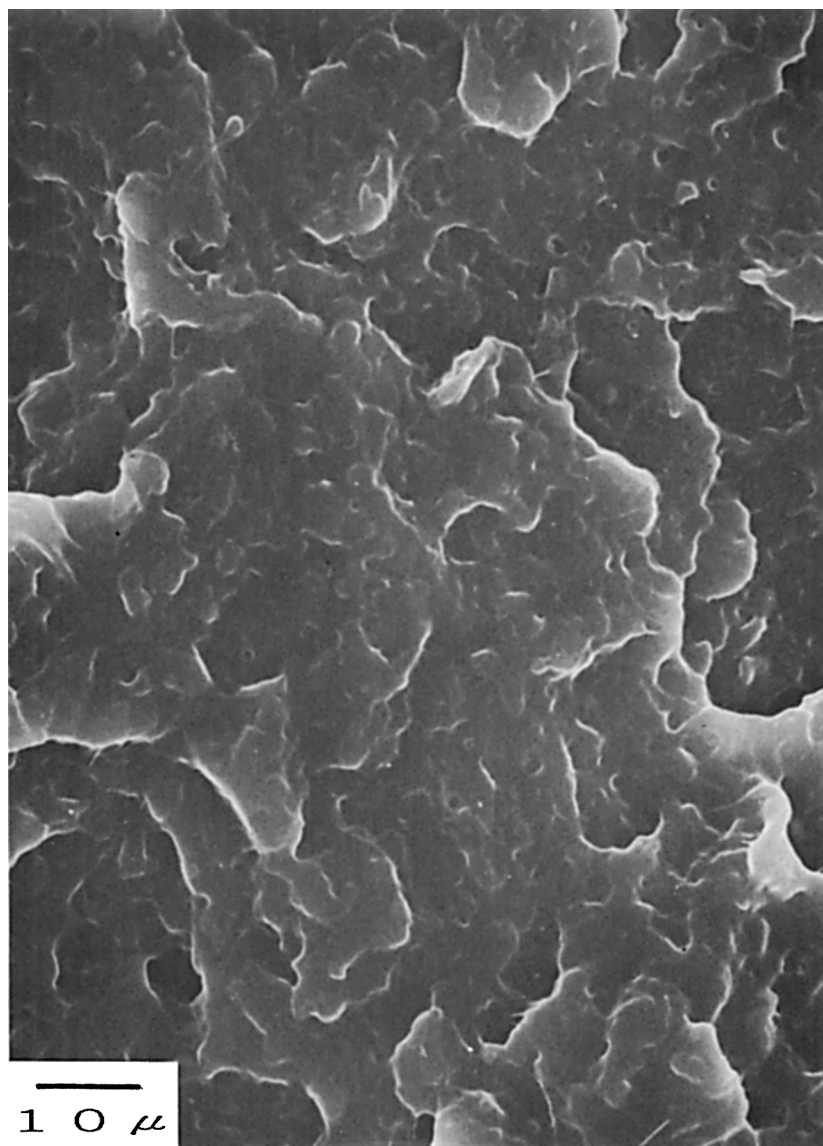


Figure 9 (Continued from the previous page)

yield strength and rigidity. On the other hand, decreases in elongation and impact strength occur.⁸

Figure 6 shows crystallization curves measured by DSC. The times to reach the noncrystallinity of 50% were 167 s for the nonnucleated block PP-A, 48 s for the talc-added block PP-B, and less 38 s for the ethylene-rich talc-added block PP-C. These data on crystallization velocity show the effects of talc addition and ethylene content as described above.

The block PP-B has the same melt viscosity and ethylene content as that of the block PP-A and also contains 0.3 wt % of talc. As shown in Table I, block PP-B does not exhibit the same annealing effect of improved impact strength even when the same heat

treatment as with block PP-A was applied. It also supports that the annealing effect on the impact strength of block PP closely relates to the crystalline structure.

(b) Effect of Ethylene Content in Talc-Added System

Block PP-C has a higher ethylene content than that of block PP-B and contains the same talc content as block PP-B. Because of its high ethylene content, block PP-C exhibits excellent TIS and Tb even when nonnucleated. As can be seen in Table I, an annealing effect for block PP-C with the same tendency

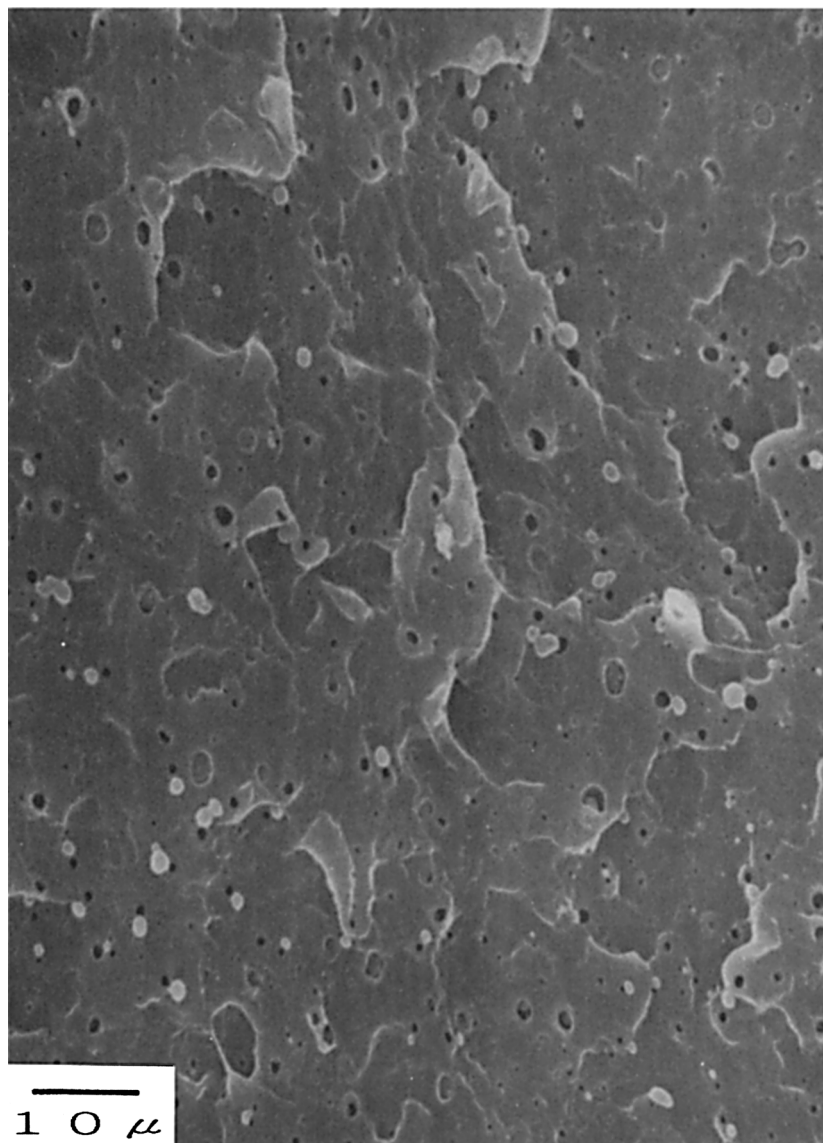


Figure 9 (Continued from the previous page)

as the talc-addition effect for block PP-B was observed. In other words, the presence of a minute amount of talc as a nucleating agent would lessen the effect of improving TIS and T_b by annealing. As for T_b , however, talc can be considered to be an additive having an improving effect without annealing.

Morphology and Fracture Model for Block PP

The improvement of impact strength of the annealed block PP, that is, the annealing effect, can be qualitatively explained by the model of the PP/PEP/

PE system with transitional layers as shown in Figure 7^{1,2} in which the domain sizes represent block PP-A. The dots at the PP/PEP and PEP/PE interfaces in Figure 7 show the concentration of PEP crystal in the transitional layer formed by annealing.

The PP matrix initially has a two-phase structure consisting of a nearly perfect crystalline portion and an amorphous portion with disordered molecular chains, but by annealing, the progress of molecular chain rearrangement would induce rejection of some amorphous portions in between lamella crystals or out of lamella crystal regions, so as to form amorphous regions on spherulite surfaces with less restriction.⁹⁻¹² Such reduced restriction in the amor-

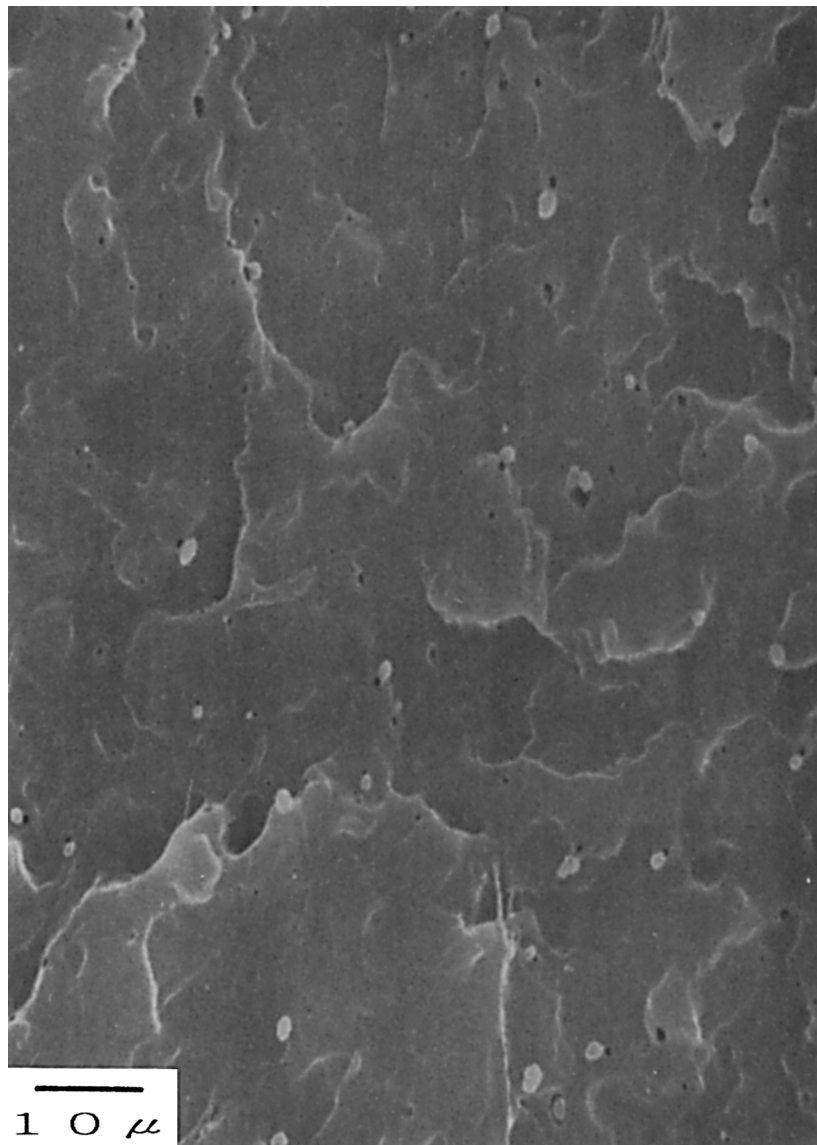


Figure 9 (Continued from the previous page)

phous component due to the recrystallization leads to the improvement in T_b . On the other hand, the partially crystalline PEP domain, by annealing, would produce the relatively thick transitional layers (a few thousand or more angstroms thickness) at their interface with the PP matrix and the PE core.^{13,14}

The thick transitional layer may be basic regardless of an interpenetration of macromolecular segments because the thickness of the interface between immiscible polymers is normally a few tens angstroms according to the thermodynamics. The thick transitional layer seems to be a phenomenon at the

interface caused by the recrystallization and the polymer diffusion promoted by the convection or the thermal expansion during annealing. The transitional layer would be difficult to extract with hot *n*-heptane. Such thickening of the interfacial zone would effect an increase in the breaking strength of the PP/PEP and PEP/PE interfaces and, hence, an improvement in TIS.

In the morphology consisting of a core-shell structure in Figure 7, the critical regions for craze formation are located at the equator of the particle (the equator being perpendicular to the applied stress).¹⁵ Based on this model, an equation to ex-

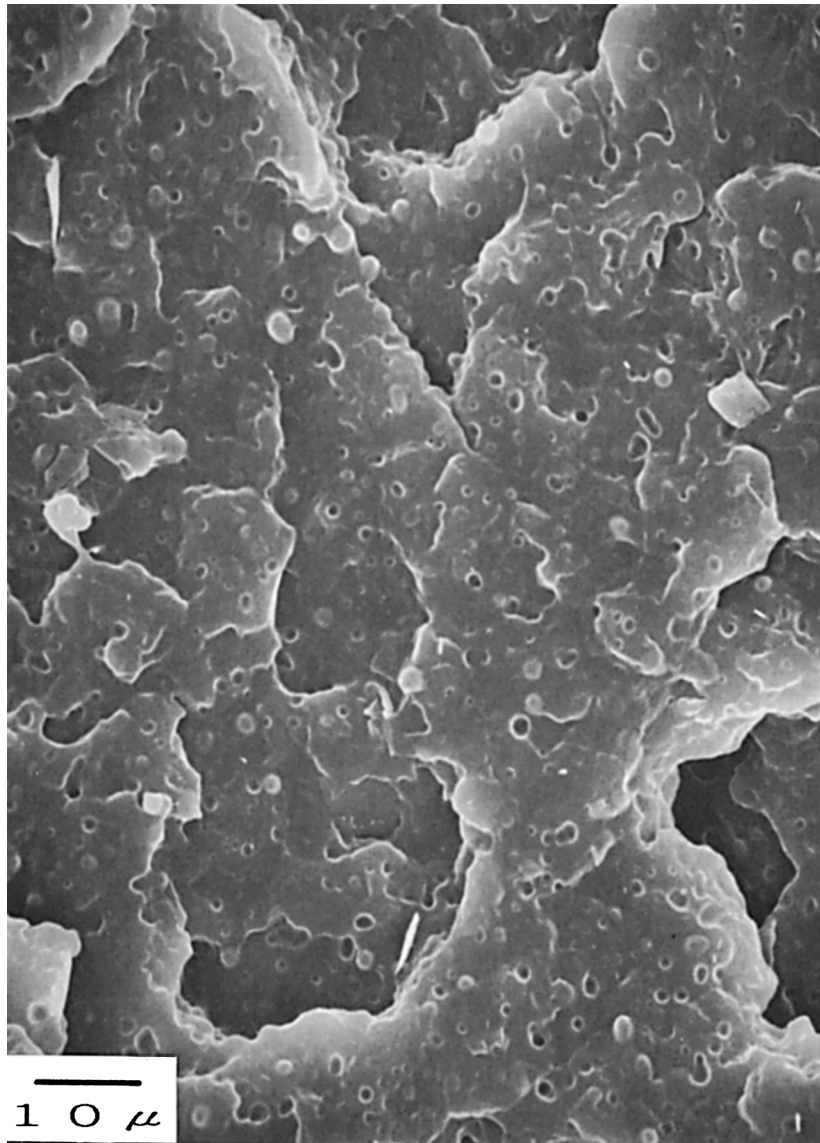


Figure 10 SEM of fracture surfaces of TIS test pieces for block PP-B: (a) unannealed; (b) annealed at 140°C for 3 h.

press the annealing effect on impact strength can be derived as follows:

$$Wb = (\sigma_m + \sigma_m^*) + (\sigma_i + \sigma_i^*) + \sigma_e \quad (1)$$

where Wb represents impact stress; σ_m , energy consumed for breaking of the PP matrix, and σ_m^* , change of σ_m by annealing; σ_i , energy required for destruction of the interface between the PP matrix and PEP dispersion, and σ_i^* , the change by annealing; and σ_e , energy consumed for deformation, or as heat, by the PEP dispersion including the PE domain.

The degree of annealing, therefore, is expressed by $(\sigma_m^* + \sigma_i^*)$ in eq. (1).

First, the effect of talc addition on the behavior of TIS on annealing will be discussed. As shown in Table I, the values of the annealing effects $(\sigma_m^* + \sigma_i^*)$ for the TIS test pieces heat-treated at 140°C for 3 h are observed to be 51 kg cm/cm² for block PP-A and 14 kg cm/cm² for block PP-B; meanwhile, the changes in crystallinity are an increase of 2.9% (= 59.7% - 56.8%) for block PP-A and an increase of 7.6% (= 65.3% - 57.7%) for block PP-B. It is understood from this finding that the difference in recrystallization of a PP matrix is strongly related

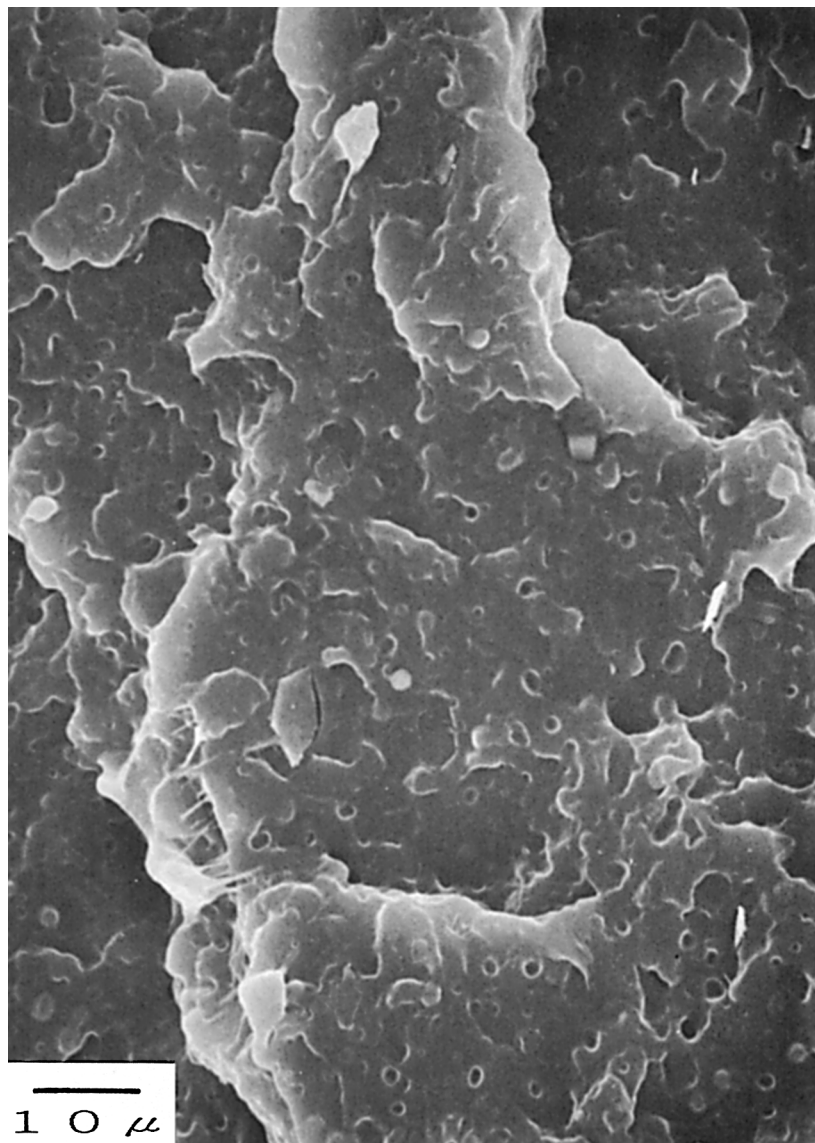


Figure 10 (Continued from the previous page)

to the outcome of the annealing effect on TIS. Two relations as follows would be presumed: In a system containing talc as a nucleating agent, recrystallization of the PP matrix would prevail. The diffusion velocity of the polymer into crystallites would be less, and, hence, the increase in the thickness of the PP/PEP transitional layer would also be less. The annealing effect with a system containing talc in the same way as with a nonnucleated PP would be exhibited so that marked progress in crystallization of the PP matrix would increase the minus value of σ_m^* so much as to make the change in TIS very small or of a minus value.

Next, the effect of talc addition on the behavior of Tb on annealing will be discussed. Figure 8 shows the relation between Tb and crystallinity for block PP-A and block PP-B. The Tb values appear in the order of the crystallinity, indicating that Tb is reduced with the progress in the crystallization of the PP matrix. On annealing at 140°C for 3 h, block PP-A and block PP-B reach nearly equal Tb values in spite of the great difference (5.6%) in their crystallinities. In the annealing of the nonnucleated block PP-A, it is postulated that formation of the amorphous phase in the PP matrix closely related to Tb was nearly complete. On the other hand, in

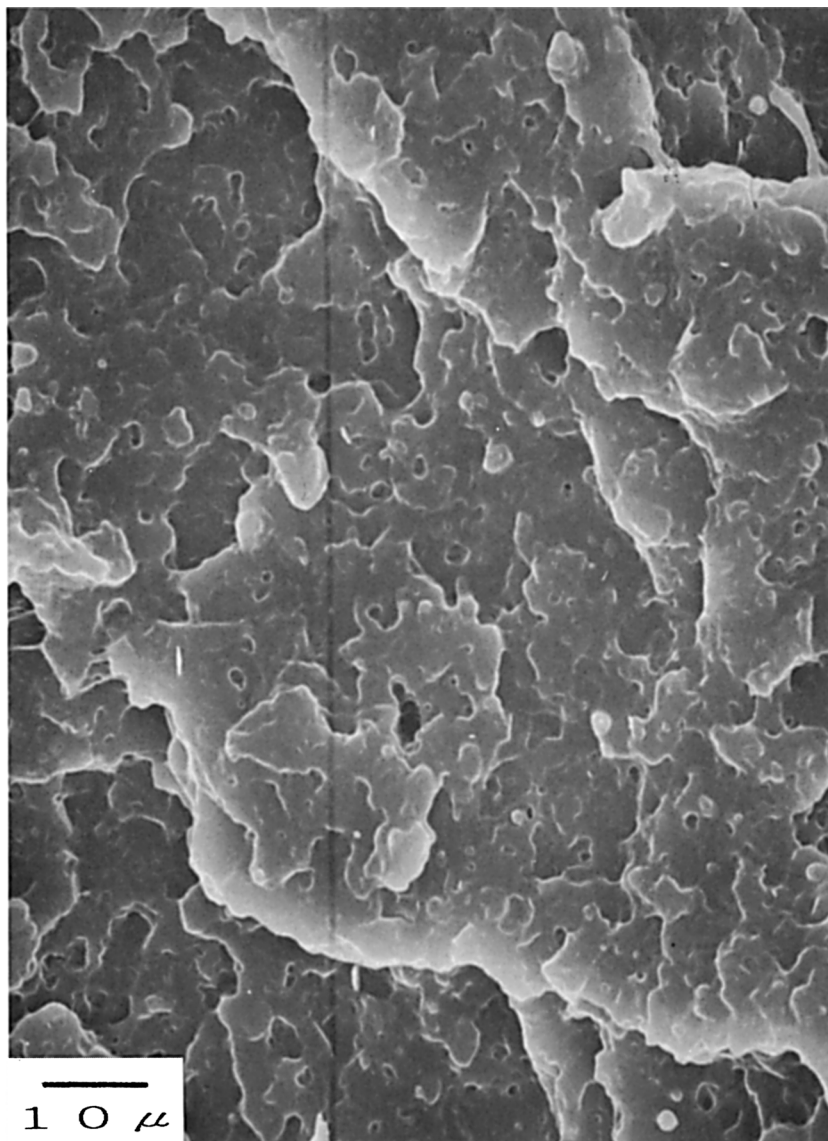


Figure 11 SEM of fracture surfaces of TIS test pieces for block PP-C: (a) unannealed; (b) annealed at 140°C for 3 h.

the annealing of the talc-added block PP-B, it is postulated that crystallization in spherulites, which does not directly contribute to brittle fracture, progressed further.

Observation of Fracture Surface of TIS Test Pieces

After determination of TIS at room temperature, the fracture surface of the test piece was observed by SEM. Figure 9 shows the fracture surface of block PP-A. On the fracture surface of the specimen before

heat treatment in Figure 9(a), there are found numerous PEP particles of about 2–3 microns in diameter; but on that of the specimen annealed at 140°C for 3 h in Figure 9(b), the existence of PEP particles is very hard to recognize. To make further confirmation, the test pieces after fracture testing were subjected to an extraction with *n*-heptane in nitrogen for 13 h and then to an observation of the fracture surface in the same manner as above, to obtain the results as shown in Figure 9(c) and (d). The dispersed particles of about 1–2 microns observed in both the photographs represent the PE

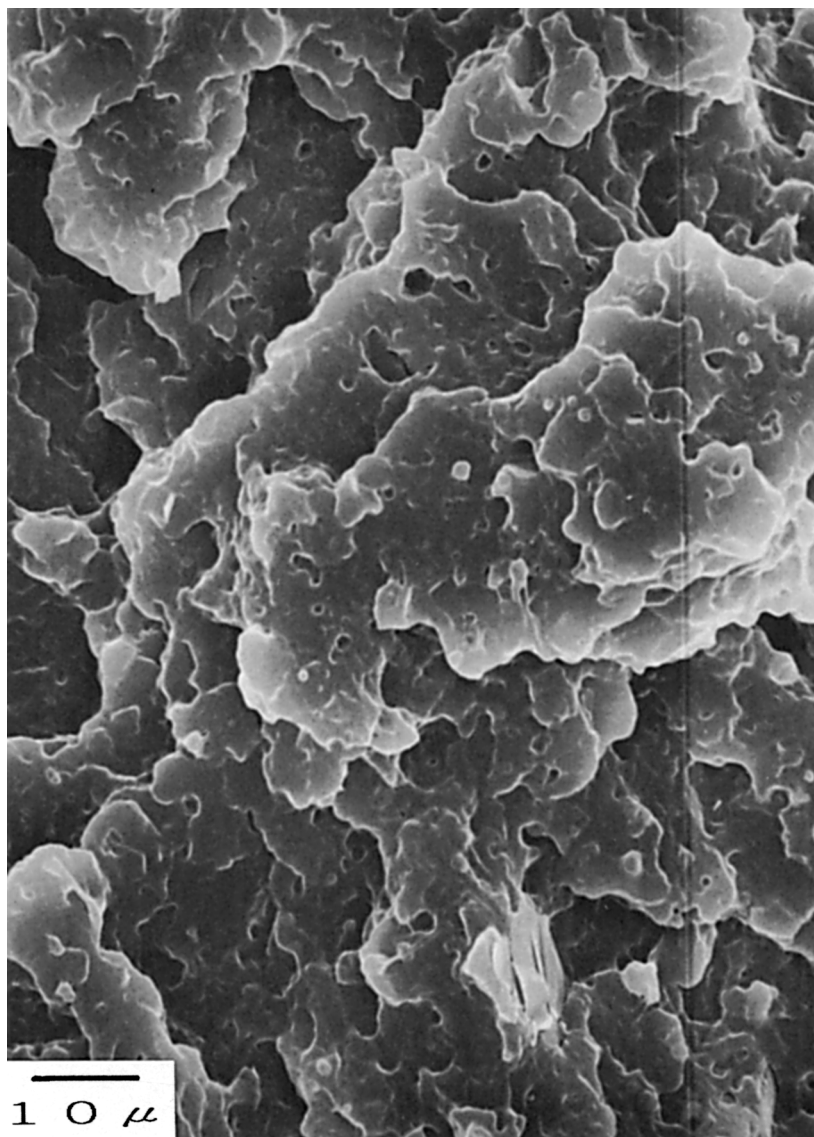


Figure 11 (Continued from the previous page)

particles that originally existed in the PEP domain and remained without being extracted. It can be confirmed that the number and size of voids corresponding to the extracted PEP phase markedly decrease on the *n*-heptane-extracted fracture surface of the specimen annealed [Fig. 9(d)] as compared with that of the unannealed specimen [Fig. 9(c)]. It can be presumed from the model of the disperse phase of annealed block PP-A in Figure 7 that the existence of PEP particles may become hard to recognize, if the fracture is advanced at the inner interface of the transitional layer because of increasing of the bonding strength of the annealed polymer interface.

On the other hand, Figures 10 and 11 show the fracture surfaces of the TIS test pieces of block PP-B and block PP-C, each containing a minute amount of talc, respectively. The marked changes in the number and size of the PEP domains before and after annealing are not discernible in Figures 10 and 11. Likewise, as related to the difference in the ethylene content of block PP, the appearance of the PEP dispersion phase did not differ before and after annealing. Figures 10 and 11 thus support the understanding of the authors regarding the crystallization behavior and polymer diffusion on annealing of a talc-added system as related to the TIS of block PP-B and block PP-C, respectively.

CONCLUSIONS

Commercial block polypropylene, a composite of PP, PEP, and PE, exhibits an annealing effect much analogous to that for a blend of these components. Annealing of moldings is effective as a means of improving impact strength and hardness, at the same time, of a block PP. The impact strength improved by annealing is stably maintained for a long period of time, although with a little drop at the initial stage.

The annealing effect on impact strength is estimated to come from the phenomenon that with the recrystallization of the matrix PP the amorphous component is rejected to outside of the lamella crystal region so as to decrease the glass transition temperature of the whole composite¹⁶ and the effect of thickening of the transitional layers caused by the mutual thermal diffusion of polymers in the interface between the PEP domain and the matrix PP.

The nucleating action of talc reduces the annealing effect on TIS, because it induces preferentially recrystallization of the matrix PP so as to hinder the mutual thermal diffusion on annealing.

The annealing effect for commercial block PP is interesting as a technique to improve the impact strength and the hardness simultaneously. Furthermore, the balance between the impact strength and the hardness can be widely controlled using a nucleating agent.

REFERENCES

1. J. Ito, K. Mitani, and Y. Mizutani, *J. Appl. Polym. Sci.*, **29**, 75 (1984).
2. J. Ito, K. Mitani, and Y. Mizutani, *J. Appl. Polym. Sci.*, **30**, 497 (1985).
3. M. Kojima and J. H. Magill, *J. Appl. Phys.*, **45**, 4159 (1974).
4. R. Greco and G. Ragosta, *J. Mater. Sci.*, **23**, 4171 (1988).
5. M. Kojima, *J. Macromol. Sci. Phys.*, **B19**, 523 (1981).
6. T. Shimonazzi, *Pure Appl. Chem.*, **56**, 625 (1984).
7. I. I. Rubin, in *Handbook of Plastic Materials and Technology*, Wiley, New York, 1990, p. 433.
8. I. I. Rubin, in *Handbook of Plastic Materials and Technology*, Wiley, New York, 1990, p. 773.
9. N. Okui and T. Sakai, *Netsushori*, **26**, 74 (1986).
10. T. G. Ryan and P. D. Calvert, *Polymer*, **23**, 877 (1982).
11. M. Tirrell, *J. Chem. Phys.*, **75**, 5194 (1981).
12. J. Menczel and J. Varga, *J. Therm. Anal.*, **28**, 161 (1983).
13. M. Kryszewski, A. Galeski, T. Pakula, and J. Grebowicz, *J. Colloid Interface Sci.*, **44**, 85 (1973).
14. T. Inoue, *Nihon Rubber Kyokai-shi*, **54**, 285 (1981).
15. T. Ricco, A. Pavan, and F. Danusso, *Polym. Eng. Sci.*, **18**, 774 (1978).
16. L. C. E. Struik, *Polymer*, **28**, 1521 (1987).

Received October 14, 1991

Accepted January 23, 1992